Modified Threshold-based Spectrum Sensing Approach for VANETs

Narendrakumar Chauhan[1], Purvang Dalal[2]
[1]Electronics and Communication Department
D. D. University
Nadiad, Gujarat, India
nvc.ec@ddu.ac.in
[2]Electronics and Communication Department
D. D. University
Nadiad, Gujarat India
pur_dalal.ec@ddu.ac.in

Abstract— The Primary User (PU) signal detection in Cognitive Radio (CR) is crucial and is achieved through spectrum sensing techniques. The Energy Detection method is a commonly used technique, and selecting a proper threshold is essential to enhance the efficiency of the CR system. This research paper demonstrates the maximum achievable throughput and validates a Modified Threshold (MT) approach. The authors consider a scenario with multiple antennas at the receiver, where these antennas are correlated and subjected to mobility effects, and they employ the Energy Detection (ED) for spectrum sensing. The study analyzes the system's performance over a Nakagami-m fading channel, considering available correlations among the antenna elements. To compute important statistical values, the Moment Generating Function (MGF) method is employed. The research employs specialized mathematical functions, such as the Lauricella and confluent hypergeometric functions, to derive closed-form expressions for the Probability of Detection when employing the diversity technique. The results indicate a significant enhancement in the performance of the proposed algorithm when utilizing the modified threshold parameter across a wide range of Signal to Noise Ratio (SNR) values. Additionally, increasing the number of branches in the antenna system further improves detection performance. Interestingly, under high fading parameter conditions (m=4), the detection probability is found to be superior with exponential correlation among the L antenna elements compared to other available correlated branches.

Keywords- Achievable Throughput, Vehicular Ad hoc Network, Correlation, Missed-detection probability, MGF

I. INTRODUCTION

Over the past times, the rapid advancement of wireless communication has led to a notable challenge: accommodating a growing multitude of wireless devices within a limited spectrum bandwidth. CR presents a solution by enabling Secondary Users (SUs) to utilize licensed frequency bands when PU is inactive. Among the available techniques, the ED method is widely favored for spectrum sensing [1]. Nevertheless, the performance of ED is significantly compromised when dealing with low SNR levels. Studies suggest that the precision of spectrum sensing largely depends on choosing the right threshold. Enhancing the effectiveness of spectrum sensing can be achieved by incorporating a greater number of antennas within the confined space of wireless devices. Due to the minimal spacing between adjacent antenna elements, the emergence of correlation among these elements is essentially unavoidable [2]. This correlation can manifest as uniform, exponential, or arbitrary, contingent upon the arrangement of the antenna branches. The evaluation of parameters like Probability of Detection (Pd), Probability of False Alarm (Pf), and Probability of Miss-detection (Pm) provides insight into the performance of spectrum sensing. Additionally, the efficiency of spectrum sensing is influenced by both the total count of antenna branches and the impacts of multipath fading [3]. The characteristics of multipath fading differ based on the specific diversity combining technique employed. Among the available diversity techniques, MRC stands out as the optimal choice due to its superior performance, even though it entails a more intricate algorithm and a prerequisite for knowledge about the channel's state compared to EGC and SC diversity [4].

This article examines the performance of detection in the context of MRC using the suggested MT [35]. In order to simplify the process, a total of 20 samples (N) are employed. The article also demonstrates impact of MT on achievable throughput. Moreover, the influence of correlation, and SNR on detection efficiency when employing the MT is also demonstrated. The authors adopt the Nakagami-m fading channel for their analysis due to its relevance in both indoor and outdoor environments. It's worth noting that by appropriately configuring the Nakagami factor m, this channel model can simulate conditions akin to Rayleigh and Rician fading channels [4].

The subsequent parts of the article are outlined as below. The section-II covers an exploration of pertinent literature. The section-III introduces the Impact of MT on achievable throughput. Elaboration on the system and signal model is presented in the section-IV. The section-V encompasses a

discussion of the simulation setup and methodology. The culmination of the study is encapsulated in the section-VI.

II. RELATED WORK

Diverse spectrum sensing techniques have been thoroughly examined and compared in [6]. Of these methods, ED has garnered significant attention despite its limitations. Research efforts have been dedicated to improving ED's performance, particularly in low SNR conditions, as evident in [9] [10-12][23]. In the presence of noise, Urkowitz investigated signal identification using ED [7]. This method involves squaring and integrating energy samples of the received signal, then comparing them against a decision threshold. However, NU impacts the determination of the threshold parameter.

Researchers in [10] stretched the work of [7] by calculating average probability of detection. They explored various fading channels to develop closed-form expressions for Pf and Pd. In [11], equations for average Pd were derived under Independent and Identically Distributed (i.i.d.) conditions for combining techniques like EGC, SC, and SSC, within a Rayleigh fading channel. [12] expanded this to include SLC. Notably, [10-12] employed a single threshold approach, limiting effectiveness in low SNR scenarios. [8] examined ED, Wavelet-based Detector (WD), and Cyclo-stationary Feature Detector (CSFD) for single-carrier signals. [9] extended this to multi-carrier signals with a single threshold, demonstrating reduced efficacy in low SNR conditions. [1] improved on [9] by introducing an adaptive double threshold approach, outperforming the single threshold in [1]. However, the double threshold used in [9] is non-dynamic, yielding suboptimal performance.

Closed-form expressions for average detection probability ($\overline{Pd}$) were derived for i.i.d. diversity branches, detailed in [13-16]. [17] established closed-form expressions for 2, 3 and 4 number of antenna branches in SLC. [18] explored the Independent but Non-identically Distributed (i.n.i.d.) branches, considering constant correlation. The impact of uniform correlation over the Nakagami-m fading channel was studied in [19]. While [3] assumed static users with correlated antennas over Nakagami-m fading channels, exponential correlation was found superior to uniform correlation in accuracy. Note that this work had limited scope in terms of antenna branches. Additionally, [34] and [35] applied the MT approach to enhance ED's detection efficiency for 2*2 MIMO and multi-carrier signal respectively, without investigating its impact on throughput.

All the mentioned studies focus on stationary users, limiting direct applicability to Vehicular Ad-Hoc Networks (VANETs). [20] computed Pf and Pm without effect of correlation between antenna branches. [21] investigated arbitrary correlation for a dual antenna receiver. In [4], closed-form Pd expressions were derived for L antennas using a ST. ED's compromised detection performance at low SNR due to NU necessitates a dynamic threshold mechanism is addressed in [4].

To our knowledge, no prior attempt has enhanced ED performance through a modified threshold in the context of VANETs, as presented in [4]. Moreover, the impact of Modification in the threshold is not investigated on the achievable throughput. In consideration of these factors, authors investigated the impact of MT on the achievable throughput. Moreover, detection performance for MRC with all possible correlations using the MT approach is also investigated.

III. IMPACT OF MODIFIED THRESHOLD ON THROUGHPUT

In [23], a Markov model is introduced to tackle the challenge of detection performance. The calculation of the upper threshold (UT) and lower threshold (LT) is achieved through the utilization of Equations (1) and (2) [34].

$$UT = \left(\frac{2}{N}Q^{-1}(Pf) + 1\right) * NU \tag{1}$$

$$LT = \left(\frac{2}{N}Q^{-1}(Pf) + 1\right) * \frac{1}{NU} \tag{2}$$

Where, NU be the Noise Uncertainty in dB (vary from 0.5 dB to 1 dB for spectrum sensing) [33].

As NU becomes more pronounced, the gap between the double threshold parameters widens to prevent instances of missed detections as depicted in Figure 1 and Figure 2. As a result, the implementation of ED with the adaptive double threshold demonstrates improved performance at low SNR. However, it's important to note that employing the double threshold mechanism leads to an extended sensing time, rendering it unsuitable for spectrum sensing.
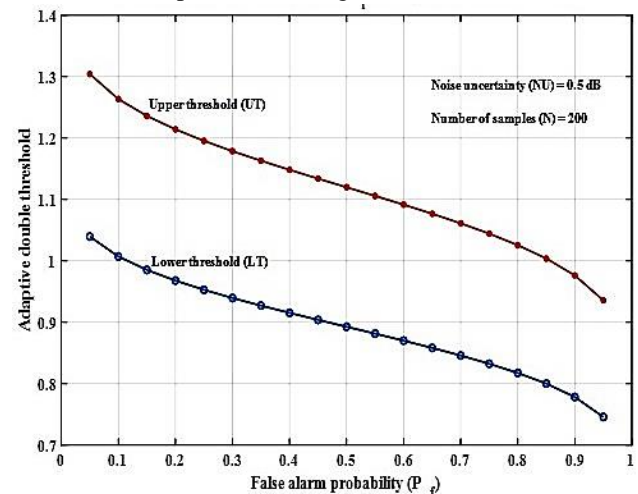

Figure 1 Impact of NU = 0.5 dB on Adaptive Double Thresholds

Building upon the concepts mentioned earlier, the research presented in [35] introduces a method to establish a fixed threshold parameter through the utilization of the adaptive double threshold. This involves operations such as addition, subtraction, calculation of the mean, and determination of the median value based on UT and LT.
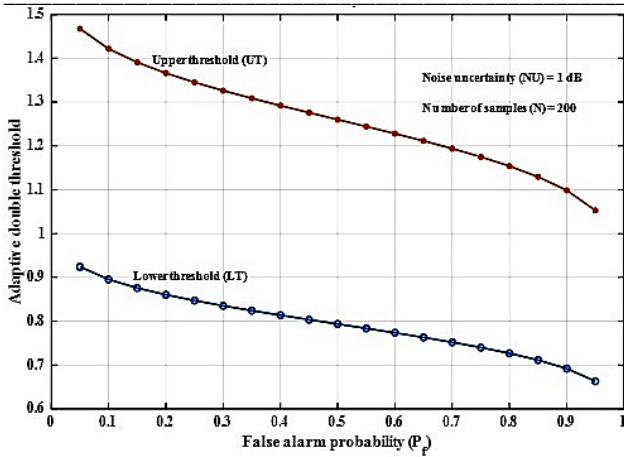
2136

Figure 2 Impact of NU = 1 dB on Adaptive Double Thresholds

It's important to highlight that utilizing the mean, median, and subtraction methods results in threshold values consistently lower than Uʎ, thereby enhancing the effectiveness of the detection performance.

Figure 3 illustrates the fluctuation in the computed threshold across a Pf range from 1 to 0.0001. This analysis pertains to a random environment with a single user and an NU value of 1 dB. Similar to the observations in Figure 3, the application of mean, median, and subtraction methods has resulted in a reduction of the threshold value. This reduction inherently contributes to enhanced detection performance. Additionally, it's noteworthy that among all the calculated thresholds during simulations in a random scenario, the intelligently determined value of subtraction (ʎs) is the lowest. This aspect underscores the choice of utilizing ʎs as the modified threshold parameter to bolster detection performance within the context of VANETs.
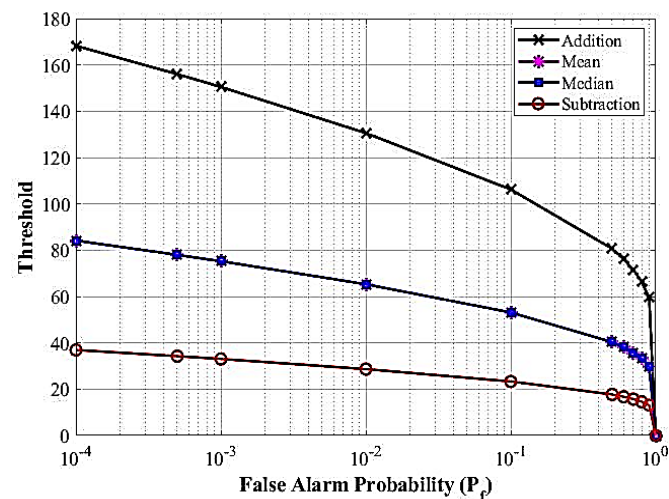

Figure 3 Comparision of proposed Thresholds

A separate series of simulations is conducted to assess the influence of NU on the parameter ʎs. The outcomes are depicted in Figure 4, illustrating the shifts in thresholds across a predefined Pf range.
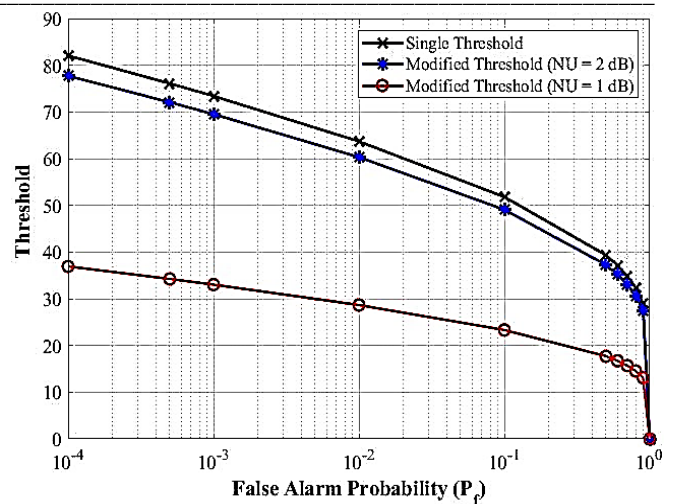

Figure 4 Assessment between ST and MT

It has been noted that as NU escalates, the value of ʎs tends to approach the values obtained from the static threshold. Importantly, it's worth mentioning that the value of ʎs consistently remains lower than static threshold. Consequently, employing ʎs serves as a safeguard for maintaining performance when utilizing ED even in scenarios with unfavorable conditions.
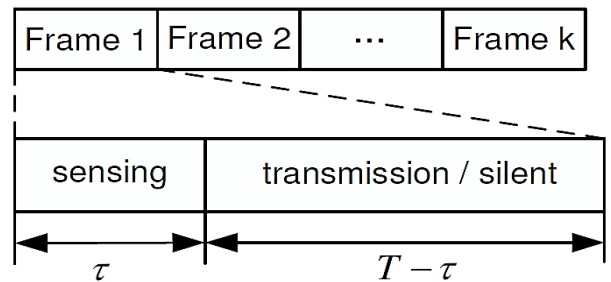

Figure 5 Frame Structure of Periodic Spectrum Sensing

As discussed earlier, the sensing time is also one of the prime performance indicators. The sensing approach should offer higher throughput with lower sensing time. The sensing time depends on the N. As we increase the N, more time will be taken by the sensing approach to sense the spectrum and hence offer less achievable throughput for the SUs. As given in [36], the N=τfs; with fs denoting the sampling frequency. The average throughput is given by equation (3).

$$R(\tau) = R_0(\Lambda, \tau) + R_1(\Lambda, \tau)$$

$$(3)$$

where,

$$R_0(\Lambda, \tau) = \frac{T - \tau}{T} C_0 (1 - Pf(\Lambda, \tau)) P(H_0)$$

$$(4)$$

$$R_1(\Lambda, \tau) = \frac{T - \tau}{T} C_0 (1 - Pd(\Lambda, \tau)) P(H_1)$$

$$(5)$$

C_0 and C_1 represent the Shannon capacities of the SU network under two different scenarios: when the PU is active and when it's inactive, with corresponding probabilities $P(H_0)$ and $P(H_1)$. The term "$T - \tau$" denotes the duration of data transmission, with "τ"

2137

representing the sensing slot, as depicted in Figure 5. The optimization problem can be given as:

$$\max \tau \quad R(\tau) = R_0(\tau) + R_1(\tau)$$
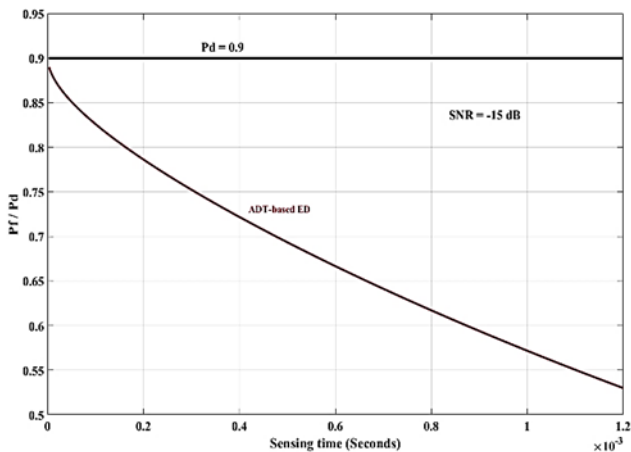$$subject \ to: \ Pd(\Lambda, \tau) \geq \overline{Pd}$$

(6)

Figure 6 Sensing Time Analysis for ADT Approach

It is assumed that the PU follows the Circularly Symmetric Complex Gaussian (CSCG) process with SNR=-15 dB and the fs is 30.72 MHz. Additionally, it is presumed that the sensing channel experiences Rayleigh fading with a fading parameter of 0.2. The SNR for SU transmission is 20 dB. The $P(H_1)$ is set at 0.2, and the desired Pd is 0.9. The sensing operation is conducted at regular intervals, with each sensing frame lasting 10 milliseconds. The simulation shown in Figure 6 is carried out to observe the sensing time. Sensing time represents how quickly the algorithm can sense the available spectrum. We see that the sensing time is decreased with an increase in the sensing time. In continuation with the sensing time analysis, the simulation is also carried out to observe the optimum sensing time as depicted in Figure 7. Optimum sensing time indicated the maximum achievable throughput for the secondary users. We see that the ADT-based ED takes 2.94271 mS to achieve a maximum throughput of 0.00387561 Bits/Sec/Hz.

The performance of the MT is also validated in terms of the sensing time analysis as compared to the ADT-based ED approach. We see that the sensing time is decreased with the use of the MT approach with respect to the ADT approach. For specific sensing time values, the ADT-based approach introduces more false alarms to achieve Pd=0.9 as compared to the MT-based ED approach. Hence, the lesser achievable throughput by the SUs with the ST-based approach. Moreover, as depicted from Figure 8 the gap between the ADT-based approach and the MT-based approach decreases and hence the achievable throughput is increased. We observe optimal sensing time as 1.41276 mS where we achieve maximum achievable throughput by MT-based approach as depicted in Figure 9.

The MT-based approach is compared with the ADT-based approach to observe the maximum achievable throughput as shown in Figure 10. The MT-based approach takes 1.41276 mS to achieve the maximum throughput of 0.0178337 Bits/Sec/Hz while the ADT-based approach takes 2.94271 mS to achieve a maximum throughput of 0.00387561 Bits/Sec/Hz. Hence, the transmission opportunity is more in the MT-based ED approach as it takes less sensing time. Moreover, the throughput is fallen down after the optimal sensing time. The simulations are carried out by taking the
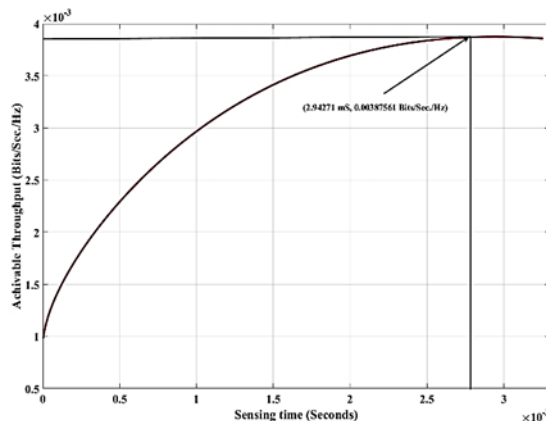

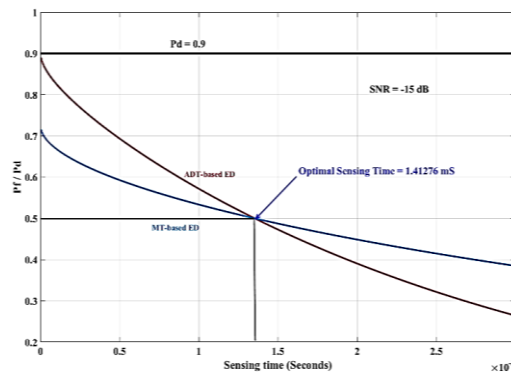Figure 7 Maximum Achievable Throughput for ADT Approach
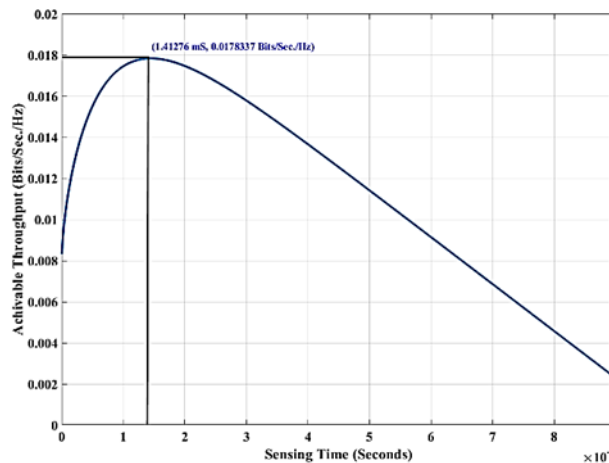

Figure 8 Sensing Time Comparison

Figure 9 Achievable Throughput with MT

SNR=-15 dB. Moreover, as the SNR increases the detection efficiency is also improved with lesser sensing time and the higher achievable throughput.
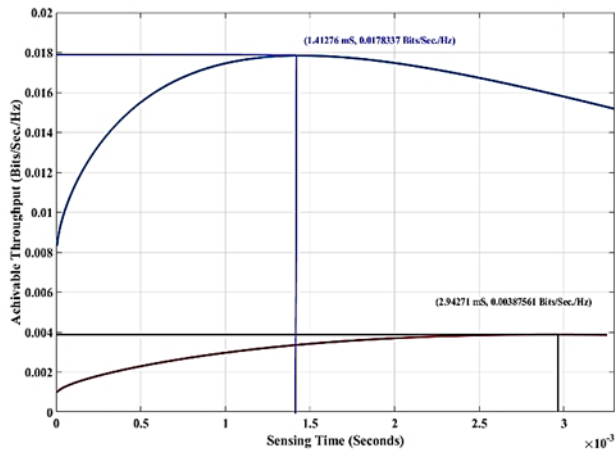
2138

_____

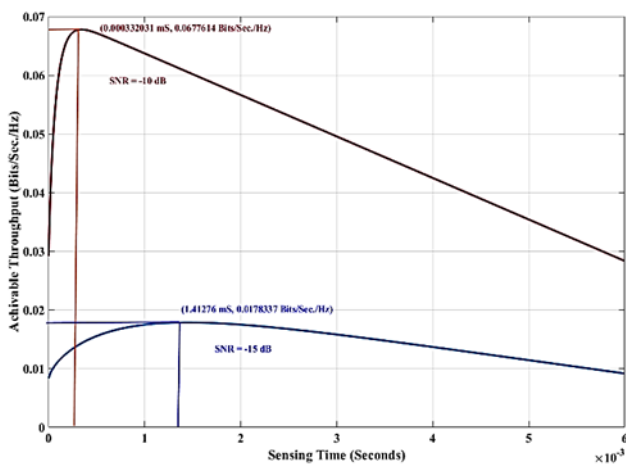Figure 10 Achievable Throughput Comparison

Figure 11 Impact of SNR on Achievable Throughput

To check the impact of the SNR on the achievable throughput, we simulate by taking the higher value of SNR and comparing it with the simulation presented in Figure 17. As depicted from Figure 11, we see the required sensing time for the higher value of SNR is lesser, and hence the SU will have a higher throughput. Consequently, the detection efficiency is also improved with the MT-based detector as it introduces the lesser Pf compared to the ADT-based detector.

To demonstrate the benefits, we compare the effectiveness of the detector with the modified threshold to the method outlined in [4], which utilizes a fixed threshold. To enhance understanding, the following section provides a concise overview of the system model employed in the simulation as described in [4].

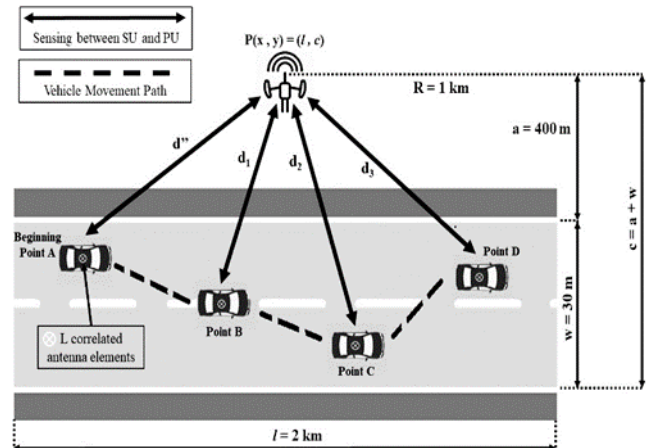## IV. SYSTEM MODEL

A. Network and Signal Model

Figure 12 Network model

To illustrate the efficacy of the MT, simulations are conducted within the VANET setting elucidated in [4]. As depicted in Figure 12, the SU vehicle begins its route from location A to D. The road's dimensions are indicated by "w" for width and "l" for length. The symbol "d" signifies the initial distance between the vehicle and the PU, while d_1, d_2, and d_3 represent the distances from the PU at points B to D respectively. The SU vehicle is armed with "L" antennas and engages in communication via a Nakagami-m fading channel.

The contest of spectrum sensing can be elucidated using a binary hypothesis. This binary hypothesis is employed to distinguish between the H_0 and H_1 of a primary user. Assuming that the SU is within the operational range of the PU, the signal received by the ith antenna is mathematically described in Equation (7):

$$y_i(t) = \begin{cases} n_i(t) & if \ \ H_0 \\ h_i(t)x(t) + n_i(t) & if \ \ H_1 \end{cases}$$

(7)

Where, $n_i(t)$ is an Additive White Gaussian Noise (AWGN) with x(t) be the diffused signal, $h_i(t)$ is the channel gain between PU and SU and defined in Eq. (8) [24]:

$$h_i(t) = \frac{g_y}{\sqrt{1 + d_b^\alpha}}$$

(8)

In this context, the symbol g_y signifies the gain associated with a Nakagami-m channel, while "α" corresponds to the factor representing path loss an outlined in [25]. Furthermore, "d_b" stands for the probability distribution of the distance variable "d" [26].

Table 1 illustrates the PDF of the channel, as presented in [4], considering various correlation schemes among the antenna branches.

TABLE 1
CHANNEL PDF FOR DIFFERENT CORRELATIONS

Uniform Correlation	$\dfrac{W}{Z}\gamma^{Lm-1}e^{-X\gamma}F_1(m,Lm;Y\gamma)$
Exponential Correlation	$\dfrac{1}{\Gamma(j)k^j}\gamma^{j-1}e^{\frac{-\gamma}{k}}$
Arbitrary Correlation	$\dfrac{2\gamma^{Lm-1}}{\Gamma(L)}\dfrac{m^{Lm}}{\varsigma}\left(\dfrac{1}{\rho}\right)^m F_1\left(m,m;Lm;\dfrac{m\gamma^2}{\varsigma}\right)$

where,

$$W = \left(\frac{m}{\bar{\gamma}}\right)^{Lm}$$

$$X = \frac{m}{\bar{\gamma}(1-\rho)}$$

$$Y = \frac{Lm\rho}{\bar{\gamma}(1-\rho)(1-\rho+L\rho)}$$

$$Z = (1-\rho)^{m(L-1)}(1-\rho+L\rho)^m\,\Gamma(Lm)$$

$$j = \frac{mL^2}{\delta}$$

$$k = \frac{\delta\bar{\gamma}}{Lm}$$

$$\delta = L + \frac{2\rho}{(1-\rho)}\left(L - \frac{1-\rho^L}{1-\rho}\right)$$

The symbol "m" signifies the Nakagami-m parameter, "ρ" denotes the correlation coefficient, "ς" stands for the mathematical expectation, and "$F_1(.,.,;)$" denotes the Lauricella hypergeometric function. This function captures the interrelation among various variables in terms of an infinite set of numbers. In this context, the hypergeometric function embodies complex dependencies on factors.

Within a VANET, it becomes crucial to examine how both the channel characteristics and the mobility factors interact, especially given the dynamic movement of vehicles. The probability density function (PDF) describing mobility, accounting for the mentioned factors, is expressed by Equation (9) as presented in reference [26].

$$f_{mo}Y(y) = \frac{d}{4lw}\left[\pi + 2arcsin\left(\frac{2(y^2-(w-c)^2)}{y^2}\right)-1\right]$$

(9)

The effectiveness of detection is determined through the combined influence of multiplying the PDF of the channel for each correlation scheme with the PDF of mobility. The PDF that encompasses both aspects, denoted as "$P_\gamma(\gamma)$" is expressed in relation to the received SNR ("γ"), taking into account the fading impact of instantaneous SNR ($\bar{\gamma}$). This relationship is outlined in Equation (10) [27].

$$\gamma \triangleq \int_0^\infty \bar{\gamma}\, P_\gamma(\gamma)\, d\gamma$$

(10)

Additionally, a Laplace transformation is applied to the variable "γ" to derive the MGF. This MGF is expressed according to Equation (11) as described in [4].

$$MGF_\gamma(t) = \int_0^\infty P_\gamma(\gamma)\, e^{t\gamma}\, d\gamma$$

(11)

To enhance performance optimization, the initial step involves calculating the first derivative of the MGF as outlined in Equation (12), employing the condition of minimizing:

$$\gamma \triangleq \frac{dMGF_\gamma(t)}{dt}\bigg|\, t = 0$$

(12)

The optimized value of "γ" is integrated with the "Marcum-Q" function in order to calculate the average detection probability. The expression for the "Marcum-Q" function is provided by Equation (13) [27].

$$Q_u\left(\sqrt{2\gamma},\Lambda\right) = 1 - e^{\frac{2\gamma+\Lambda}{2}}\sum_{n=u}^\infty\left(\frac{\sqrt{\Lambda}}{\sqrt{2\gamma}}\right)^n I_n\left(\sqrt{2\Lambda\gamma}\right)$$

(13)

To summarize, the process of obtaining the expression for average detection probability involves the following steps:

1. Calculate the channel PDF corresponding to a specific correlation scheme, using the information provided in Table 1.
2. Substituting the calculated channel and mobility PDFs into Equation 8 yields the joint PDF.
3. Perform a Laplace transform on the joint PDF to derive the MGF of the received SNR.
4. Combine the MGF of the received SNR with the Marcum-Q function (as shown in Equation 13) to compute the average detection probability.

It's important to emphasize that the MGF will vary for each correlation scheme, and thus should be applied accordingly. The average Pd for each of these correlation schemes is presented in Table 2, as derived in [4].

TABLE 2
AVERAGE *Pd*

Uniform Correlation	$\displaystyle\int_0^\infty Q_u\left(\sqrt{2\gamma},\sqrt{\Lambda}\right)\frac{A}{B}\gamma^{Lm-d}e^{-C\gamma}F_1\left(md,\frac{La}{b};C\gamma\right)d\gamma$
Exponential Correlation	$\displaystyle\int_0^\infty Q_u\left(\sqrt{2\gamma},\sqrt{\Lambda}\right)\frac{1}{Z}\Gamma(d)e^{-E\gamma}F_1(\rho,L;C\gamma)d\gamma$
Arbitrary Correlation	$\displaystyle\int_0^\infty Q_u\left(\sqrt{2\gamma},\sqrt{\Lambda}\right)\frac{\left(\frac{m}{\bar{\gamma}}\right)^{d(Lm-1)}e^{\left(\frac{-\gamma}{\bar{\gamma}(1-\rho)}\right)}*F_1\left(m,Lm;\frac{Lm*\rho d}{(1-\rho+Ld)}\right)}{(1-\rho)^{d(L-1)}\Gamma(Lm)}d\gamma$

where,

$$A = \frac{d}{\bar{\gamma}^m}$$

$$B = \frac{m}{\bar{\gamma}L}$$

2140

_____

$$C = \frac{\rho(L\rho + \rho^2)}{\bar{\gamma}(1 - \rho + L\rho)}$$

In conclusion, the closed-form expression for the average detection probability ($\overline{Pd}$) is derived through the utilization of the minimizing condition. The calculated value of $\overline{Pd}$ is found to closely approximate the theoretical value, as reported in [4]. The $\overline{Pd}$ for each of the correlation schemes is presented in Table 3 [4].

TABLE 3
CLOSED FORM OF $\overline{Pd}$

Uniform Correlation	$1 - \frac{A\Gamma(Lm+\rho)}{C\Gamma(m)}e^{\frac{-\Lambda}{2}}\sum_{n=u}^{\infty}\sum_{i=0}^{\infty}\left(\frac{\Lambda}{2}\right)^{n}\frac{\Gamma(\rho)m^{i}}{\Gamma(n+1)(1+B)^{Lm+i}i!}F_{1}\left(\rho;n+1;\frac{\Lambda}{2(1+B)}\right)$
Exponential Correlation	$\varsigma\left[G_{1} + \frac{\eta}{2}\sum_{n=1}^{u-1}\left(\frac{\Lambda}{2}\right)^{n}\frac{1}{n!}F_{1}\left(H;n+1;\frac{\Lambda k}{2(1+k)}\right)\right]$
Arbitrary Correlation	$\frac{F_{1}\left(m,Lm;Lm^{2}*\rho;\frac{\rho \times d}{\bar{\gamma}(1-2m)(1-\rho+Ld)}\right)}{2\left(\frac{\bar{\gamma}\times d}{m}\right)^{L}m(1-\rho)^{m(L-1)}} \times \sum_{n=u}^{\infty}\left(\frac{\Lambda}{2}\right)^{n}F_{1}(q,r,s,t)$

where,

$$\varsigma = \frac{1}{2^{j-1}\Gamma(j)}k^{j}$$

$$\eta = \Gamma(j)\left(\frac{2D}{1+k}\right)^{j}e^{\frac{-\Lambda}{2}}$$

$$D = \frac{\rho(L\rho + \rho^2)}{\bar{\gamma}(1 - \rho + L\rho)}$$

$$G_{1} = \frac{2^{j-1}(j-1)!}{\frac{1^{2k}}{k}}\left(\frac{k}{1+k}\right)e^{\frac{-\Lambda}{2(1+k)}}\left[\left(1 + \frac{1}{k}\right)\left(\frac{1}{1+k}\right)^{j-1}L_{j-1}\left(\frac{-\Lambda\frac{L}{\bar{\gamma}}}{2(1+k)}\right)\right.$$
$$\left. + \sum_{n=0}^{j-2}\left(\frac{1}{k+1}\right)^{n}L_{n}\left(\frac{-\Lambda k}{2(k+1)}\right)\right]$$

, and L_{n} is Lagrangian's polynomial of n degree [28].

It's important to highlight that the modified threshold (Λ_{s}) suggested in [35] is adaptable to the NU, unlike the threshold Λ employed in the above derived expressions from reference [4]. Consequently, this study focuses on the utilization of the adaptable threshold Λ_{s} with the aim of improving detection performance. The following section validates the detection performance in the presence of this modified threshold.

V. SIMULATION

A. Simulation Environment

This section provides an overview of the simulations conducted to explore and confirm the advantages of employing an adjusted threshold with the ED in VANETs. The assessment is performed under the influence of Nakagami-m fading channels. Alongside the fundamental network model detailed in Section 4, the other simulation parameters are enumerated in Table 4.

TABLE 4
SIMULATION PARAMETERS

Sr no.	Parameters	Value
1	α	0.9 and 1.9
2	m	2 and 4
3	w	30 m
4	l	2 km
5	a	400 m
6	PU protection range	1 km

B. Simulation Methodology

The initial series of simulations is conducted with the aim of contrasting the performance of ED when utilizing the modified threshold against the outcomes obtained with a fixed threshold. Throughout these simulations, we have taken into account an equal number of antenna branches for MRC diversity. The performance evaluation is undertaken for each of the correlation schemes, which encompass uniform, arbitrary, and exponential correlations.
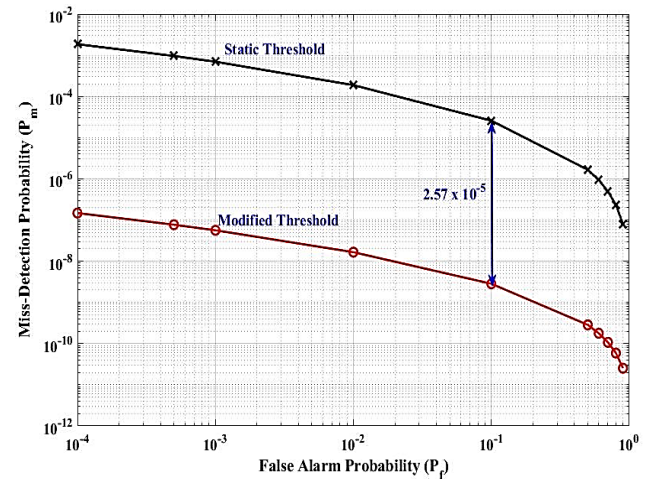

Figure 13 Comparision of ST and MT with Uniform Correlation Scheme

The subsequent series of simulations is conducted to analyze how varying factors such as the number of antenna branches (L), the Nakagami-m parameter (m), SNR, and correlation coefficient affect the improvements achieved through the implementation of the exponential correlation scheme.
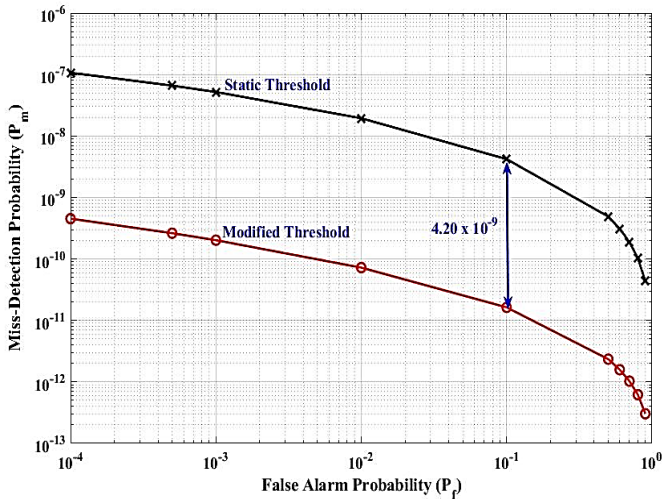
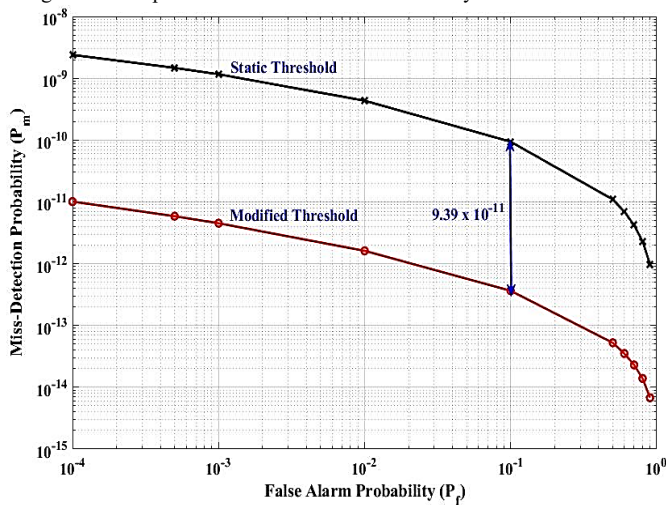Figure 14 Comparision of ST and MT with Arbitrary Correlation Scheme

Figure 15 Comparision of ST and MT with Exponential Correlation Scheme
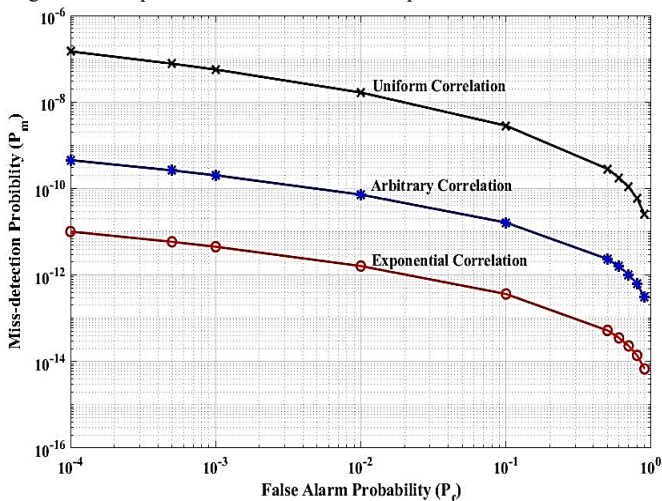

Figure 16 Comparision of all correlation schemes with MT

Figure 13, 14, and 15 illustrate the comparison between the utilization of static and modified thresholds for MRC diversity, considering uniform, arbitrary, and exponential correlation schemes. The simulations are conducted using constant values of L = 4, m = 4, SNR = 20 dB, and a correlation coefficient of 0.8. As shown in Figures 13, 14, and 15, when using the proposed threshold,

there is an additional relative improvement of approximately 2.5×10^{-5} (99.98%) with the uniform correlation scheme, 4.20×10^{-9} (99.61%) with the arbitrary correlation scheme, and 9.39×10^{-11} (99.61%) with the exponential correlation scheme in the probability of missed detection (Pm).

Figure 16 illustrates a performance comparison between the modified threshold and the correlation scheme, highlighting a reduced rate of missed detections when employing the modified threshold with exponential correlation. Figure 17 confirms that the use of the modified threshold results in superior detection performance (Pd = 1 – Pm) compared to what is observed with a static threshold.
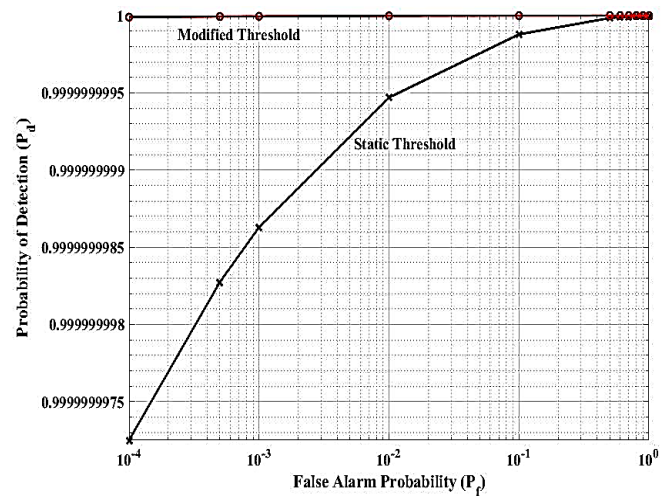

Figure 17 ROC for Exponential Correlation Scheme with ST and MT

The impact of the number of L is showcased in Figure 18 when using the modified threshold in conjunction with the exponential correlation scheme, with Pf being varied. Throughout this analysis, we maintain L = 2 and L = 4, while setting m = 4, SNR = 20 dB, and a correlation coefficient of 0.8 during the simulations. It's worth noting that having more than one antenna branch at the receiver enhances receiver diversity, leading to more accurate detection of the original transmitted signal. Consequently, augmenting the number of antenna branches can improve signal quality, although this improvement comes at the expense of increased complexity. The correlation matrix (R) for L equals to 4 is provided as indicated in [32]. It is evident that the enhancement in detection performance is notable when increasing the L.

$$R = \begin{bmatrix} 1 & 0.4318 & 0.1340 & 0.8995 \\ 0.4318 & 1 & 0.6517 & 0.0421 \\ 0.1341 & 0.6517 & 1 & 0.5484 \\ 0.8995 & 0.0421 & 0.5484 & 1 \end{bmatrix}$$
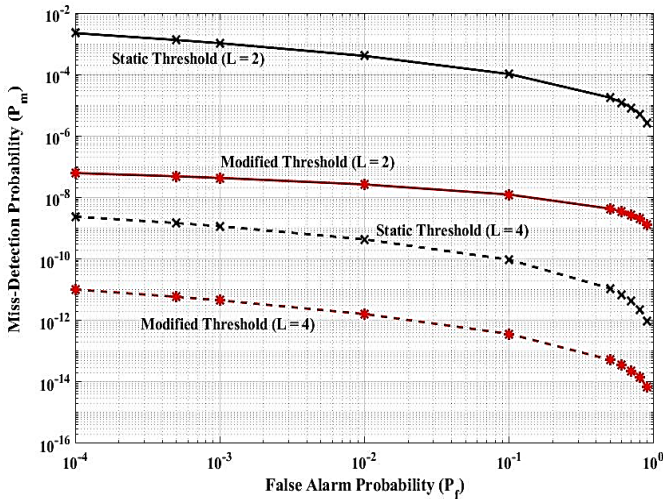
Figure 18 Effect of L on Exponential Correlation Scheme with Static and Modified Threshold

The efficiency of detection can also be enhanced by opting for a lower value of m in conjunction with a higher value of L, and conversely. To gain a deeper understanding of the influence of the parameter m, we provide a simulation in Figure 19. This simulation is conducted with L = 4, correlation coefficient = 0.8, and SNR = 20 dB.
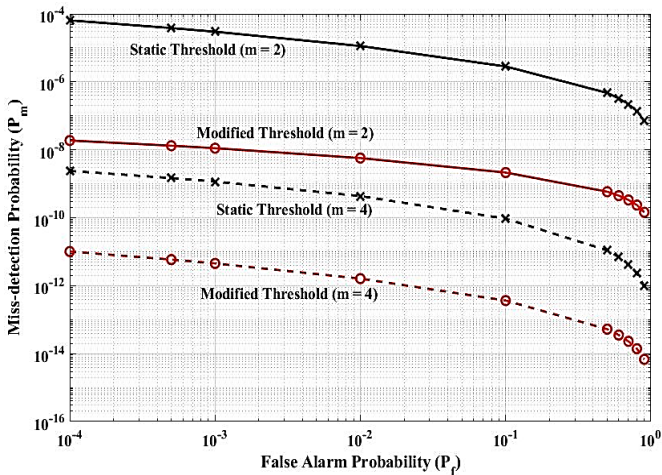

Figure 19 Effect of Nakagami-m parameter on Exponential Correlation Scheme with ST and MT

Figure 19 illustrates how the variation in the Nakagami-m parameter impacts the detection performance when utilizing the modified threshold. The detection effectiveness experiences a decrease when adopting lower values of the Nakagami-m parameter (m = 2). Conversely, a higher fading parameter (m = 4) frequently results in dynamic fading, which aligns more closely with real-world scenarios. For values of m > 4, which lead to Rician fading [30], it indicates a greater requirement for line of sight components for effective communication.

Furthermore, we examine the detection performance by introducing variations in SNR while maintaining a correlation coefficient of 0.8, as depicted in Figure 20. Additionally, we explore the impact of changes in the correlation coefficient with a fixed SNR of 20 dB, as shown in Figure 21. For these

evaluations, we have set Pf to 0.1, along with L = 4 and m = 4 as consistent simulation parameters.
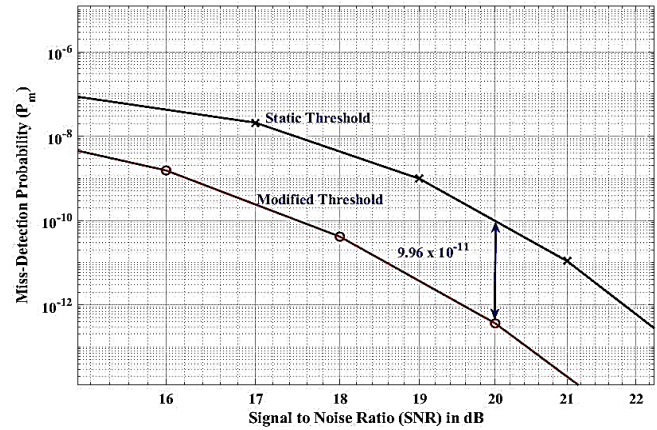

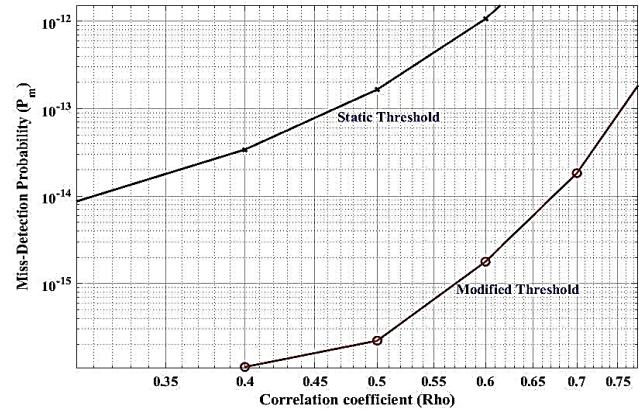Figure 20 Effect of SNR on Exponential Correlation Scheme with ST and MT

Figure 21 Effect of Correlation Coefficient on Exponential Correlation Scheme with ST and MT

The general trend observed from both Figure 20 and Figure 21 is that detection performance tends to improve with higher SNR values and lower correlation coefficients. Additionally, a noteworthy observation is that detection performance is notably influenced by correlation coefficients exceeding 0.7.

VI. CONCLUSIONS

We have demonstrated the effectiveness of the proposed Modified Threshold approach in a VANET environment. Our focus was on optimizing the Energy Detector's performance by considering MRC diversity in a Nakagami-m fading channel. It's important to note that our evaluation was limited to urban areas and doesn't apply to highway or two-lane road scenarios. Despite the improvements, the detection performance maintains its underlying behavior: the exponential correlation scheme consistently outperforms the uniform and arbitrary correlation schemes.

The simulation results yielded several key observations:

1. The MT-based approach offers higher achievable throughput with less sensing time as compared to the ADT-based Approach.
2. Improved Detection Performance: At a Probability of False Alarm (Pf) of 0.1, the modified threshold

2143

_____

significantly improved detection performance for the uniform, arbitrary, and exponential correlation schemes. Specifically, in the context of vehicular communication, it resulted in approximately 99.98%, 99.61%, and 99.61% performance gains, respectively, compared to the static threshold.

3. Comparative Improvement: When combined with the exponential correlation scheme, the proposed modified threshold scheme exhibited substantial improvements. It achieved a remarkable 99.98% and 97.76% enhancement over the uniform and arbitrary correlation schemes, respectively.

4. Mitigation of High Correlation Impact: The potential negative impact of high correlation on detection performance was alleviated by increasing the number of antenna branches (L). As a result, the performance of the Energy Detector naturally decreased with higher L values. This led to the observation that the modified threshold showed more room for improvement with lower L values. For instance, with the exponential correlation scheme and Pf = 0.1, improvements of 99.98% and 99.61% were observed for L = 2 and L = 4, respectively, compared to the Static Threshold.

5. Fading Parameter Impact: The performance of the modified threshold detector exhibited improvements across a range of fading parameters (m). Specifically, using the exponential correlation scheme and Pf = 0.1, improvements of 99.92% and 99.61% were observed for m = 2 and m = 4, respectively, compared to the Static Threshold.

6. Signal-to-Noise Ratio and Correlation Coefficient Factors: Enhanced detection performance was achieved through higher signal-to-noise ratios and lower correlation coefficient factors.

These findings collectively emphasize the effectiveness of the proposed Modified Threshold approach and its compatibility with the exponential correlation scheme for enhancing detection performance in vehicular communication within urban settings.

REFERENCES

[1] N. Chauhan, Aasnil Shah, Purav Bhatt, Purvang Dalal.: "Simulation based Analysis of Non-Cooperative Spectrum Sensing Techniques in Cognitive Radio", The Mattingley Publishing Co., Inc. 2020 ISSN: 0193-4120, pp. 5149-5162.

[2] Vegni, A.M., Agrawal, D.P.: "Cognitive vehicular networks", CRC Press Inc., Boca Raton, FL, USA, 2016.

[3] Al-Juboori, S., Fernando, X.N.: "Multiantenna spectrum sensing over correlated Nakagami- m channels with MRC and EGC diversity receptions", IEEE Trans. Vehicular Technology, 2018, 67, (3), pp. 2155–2164.

[4] S. Kavaiya, D. Patel, Yong Liang Guan, Sumei Sun, Yoong Choon Chang, Joanne Mun-Yee Lim.: "On the energy detection performance of multi-antenna correlated receiver for vehicular communication using MGF approach". IET Communication, 2020, Vol. 14 Issue 12, pp. 1858-1868.

[5] Win, M.Z., Chrisikos, G., Winters, J.H.: "MRC performance for M-ary modulation in arbitrarily correlated Nakagami fading channels", IEEE Communication Lett., 2000, 4, (10), pp. 301–303.

[6] Yucek, T., Arslan, H.: "A survey of spectrum sensing algorithms for cognitive radio applications", IEEE Communication Survey. Tutor., 2009, 11, (1), pp. 116–130.

[7] Urkowitz, H.: "Energy detection of unknown deterministic signals", Proc. IEEE, 1967, 55, (4), pp. 523–531.

[8] N. Chauhan and S. Thavalapill.: "Spectrum Sensing in Cognitive Radio for Single Carrier Signal", National Conference Computer Engineering, Information and Communication Technology, 2016, ISBN 978-93-5288-056-0, pp. 112-116.

[9] N. Chauhan and S. Thavalapill.: "Spectrum Sensing in Cognitive Radio for Multi-Carrier (OFDM) Signal", 23rd International Conference on Innovation in Electrical & Electronics Engineering (ICIEEE 2016) ISSN (PRINT): 2393-8374, (ONLINE): 2394-0697, VOLUME-3, ISSUE-9, 2016.

[10] Kostylev, V.I.: "Energy detection of a signal with random amplitude". Proc. Int. Conf. on Communications, New York, NY, USA, 2002, vol. 3, pp. 1606– 1610.

[11] Digham, F. F., Alouini, M.-S., Simon, M.K.: "On the energy detection of unknown signals over fading channels". Proc. IEEE Int. Conf. Communication, Anchorage, AK, USA, May 2003, vol. 5, pp. 3575–3579.

[12] Digham, F. F., Alouini, M.S., Simon, M.K.: "On the energy detection of unknown signals over fading channels", IEEE Trans. Communication, 2007, 55, (1), pp. 21–24.

[13] Herath, S. P., Rajatheva, N.: "Analysis of equal gain combining in energy detection for cognitive radio over Nakagami channels". Proc. IEEE GLOBECOM, Los Angeles, CA, USA, 2008, pp. 1–5.

[14] Herath, S. P., Rajatheva, N., Tellambura, C.: "On the energy detection of unknown deterministic signal over Nakagami channels with selection combining". Proc. IEEE CSECE, 2009, pp. 745–749.

[15] Herath, S. P., Rajatheva, N., Tellambura, C.: "Unified approach for energy detection of unknown deterministic signal in cognitive radio over fading channels". Proc. IEEE The Int. Conf. on Communications (ICC) Workshop, Dresden, Germany, June 2009, pp. 1–5.

[16] Herath, S.P., Rajatheva, N., Tellambura, C.: "Energy detection of unknown signals in fading and diversity reception", IEEE Trans. Communication, 2011, 59, (9), pp. 2443–2453.

[17] Banjade, V.R.S., Rajatheva, N., Tellambura, C.: "Performance analysis of energy detection with multiple correlated antenna cognitive radio in Nakagami-m fading", IEEE Communication Lett., 2012, 16, (4), pp. 502–505.

[18] Adebola, E., Annamalai, A.: "Unified analysis of energy detectors with diversity reception in generalised fading channels", IET Communication, 2014, 8, (17), pp. 3095–3104.

[19] Al-Juboori, S., Fernando, X., Deng, Y., et al.: "Impact of inter branch correlation on multichannel spectrum sensing with SC and SSC diversity combining schemes", IEEE Trans. Vehicular Technology, 2018, 68, (1), pp. 456–470.

2144

---

[20] Gahane, L., Sharma, P.K., Varshney, N., et al.: "An improved energy detector for mobile cognitive users over generalized fading channels", IEEE Trans. Communication, 2018, 66, pp. 534–545.

[21] Kavaiya, S., Patel, D.K., Guan, Y.L., et al.: "On the energy detection performance of arbitrarily correlated dual antenna receiver for vehicular communication", IEEE Communication Lett., 2019, 23, (7), pp. 1186–1189.

[22] Ying-Chang Liang, Yonghong Zeng, Edward C.Y. Peh, Anh Tuan Hoang.: "Sensing-Throughput Tradeoff for Cognitive Radio Networks", IEEE Trans. Communication, Vol. 7, No. 3, 2008, pp.

[23] Yulei Liu, Jun Liang, Nan Xiao, Xiaogang Yuan, Zhenhao Zhang, Meng Hu, Yulong Hu.: "Adaptive double threshold energy detection based on Markov model for cognitive radio", https://doi.org/10.1371/journal.pone.0177625, 2017.

[24] Ai, Y., Cheffena, M., Mathur, A., et al.: "On physical layer security of double Rayleigh fading channels for vehicular communications", IEEE Communication Letter, 2018, 7, (6), pp. 1038–1041.

[25] Kåredal, J., Czink, N., Paier, A., Tufvesson, F., & Molisch, A. (2011). Path loss modeling for vehicle-to-vehicle communications. IEEE Transactions on Vehicular Technology, 60(1), 323-328.

https://doi.org/10.1109/TVT.2010.2094632

[26] Zhu, S., Guo, C., Feng, C., et al.: "Performance analysis of cooperative spectrum sensing in cognitive vehicular networks with dense traffic". Vehicular Technology Conf. (VTC), Montreal, Canada, 2016, pp. 1–6.

[27] Simon, M.K., Alouini, M.-S.: "Digital communication over fading channels, vol. 95", John Wiley & Sons, 2005.

[28] Gradshteyn, I.S., Ryzhik, I.M.: "Table of integrals, series, and products", Elsevier, Academic Press, ISBN-13: 978-0-12-373637-6, ISBN-10: 0-12-373637-4, 2014

[29] Simon, M.K., Alouini, M.: "A unified approach to the performance analysis of digital communication over generalized fading channels", Proc. IEEE, 1998, 86, (9), pp. 1860–1877.

[30] Aalo, V.A.: "Performance of maximal-ratio diversity systems in a correlated Nakagami-fading environment", IEEE Trans. Communication, 1995, 43, (8), pp. 2360–2369.

[31] Zlatanov, N., Hadzi-Velkov, Z., Karagiannidis, G.K.: "An efficient approximation to the correlated Nakagami-m sums and its application in equal gain diversity receivers", IEEE Trans. Wireless Commun., 2010, 9, (1), pp. 302–310.

[32] Song, Z., Zhang, K., Guan, Y.L.: "Generating correlated Nakagami fading signals with arbitrary correlation and fading parameters". Proc. IEEE ICC "02, New York, NY, USA, 2002, Vol. 3, pp. 1363–1367.

[33] Lu Wei, Olav Tirkkonen.: "Spectrum Sensing in the Presence of Multiple Primary Users", IEEE Trans. Communication, Vol. 60, No. 5, 2012, pp. 1268-1277.

[34] Chauhan, N.., Kavaiya, S.., & Dalal, P. (2023). Modified Threshold - based Intelligent Enhanced Energy Detector for Cognitive Radio Networks. International Journal of Intelligent Systems and Applications in Engineering, 11(9s), 120–130.

[35] Chauhan, N., Dalal, P. (2023), "Advancement of Non-coherent Spectrum Sensing Technique in Cognitive Radio Networks - A Simulation-Based Analysis" Computing Science, Communication and Security. COMS2 2023. Communications in Computer and Information Science, vol 1861. Springer, Cham. https://doi.org/10.1007/978-3-031-40564-8_7

[36] Emara, M., Ali, H.S., Khamis, S.E.A. and Abd El-Samie, F.E., 2016. Spectrum sensing optimization and performance enhancement of cognitive radio networks. Wireless Personal Communications, 86, pp.925-941.